Journal of Materials Chemistry A

Accepted Manuscript

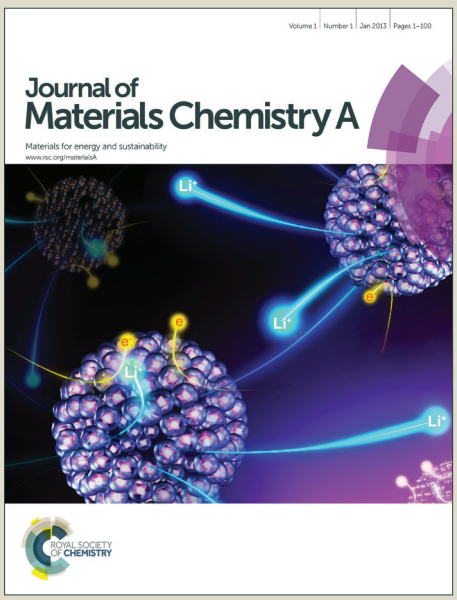

ROYAL SOCIETY OF CHEMISTRY

www.rsc.org/materialsA

Journal of Materials Chemistry A RSCPublishing

ARTICLE

Chemically Anchored Liquid-PEO based Block Copolymer Electrolytes for Solid-State Lithium-Ion Batteries

J. Rolland,[a] J. Brassinne,[a] J.-P. Bourgeois,[a] E. Poggi,[a] A. Vlad[b] and J.-F. Gohy,[a]

Cite this: DOI: 10.1039/xoxxoooooox

Received ooth January 2012,
Accepted ooth January 2012

DOI: 10.1039/xoxxoooooox

www.rsc.org/

Solid-state electrolytes are being considered the keystone element for the development of safer all-solid-state lithium-ion batteries. While poly(ethylene oxide) (PEO) solid-state polymer electrolytes are known to support a Li^+ flux, satisfying conductivities are reached only above the melting point of the PEO crystallites (> 65°C) rendering PEO unpractical. Herein, by means of block-copolymer engineering, we design a mechanically clamped liquid-PEO electrolyte that combines the high ionic conductivity of a low molecular mass PEO while retaining the dimensional integrity of a solid material. Attractive ionic conductivities of about 0.01 mS/cm are attained at room temperature without compromising mechanical properties. The electrolyte shows a wide electrochemical stability window and help in building a stable interface with lithium metal. Competitive performances are attained when integrating the developed materials into operational/functional prototype batteries highlighting the provided potential.

1. Introduction

Lithium-ion batteries (LIBs) play a crucial role in our daily life due to the increasing demand of wireless technologies, portable electronics and electric vehicles.[1]Although many achievements have been done so far to improve their performances, the challenge is still to design safer, cheaper, long lasting and high energy density, high power density batteries.[2,3] Designing better non-aqueous ion-conducting electrolytes is considered as one of the key elements in alleviating these issues. Currently, most of the commercial LIBs contain carbonate based organic liquid electrolytes given their high ionic conductivity and transference numbers in the temperature range of interest. Whereas this technology is well matured and exhibits the best performances amongst the various classes of electrolytes, it is also famous for severe safety issues: leakage of corrosive and flammable products as well as the explosion risks.[4,5]

Safety issues have been considerably alleviated through liquid electrolyte incorporation into polymer matrixes. Gel-polymer and swelled polymer membranes are the most known composite systems in this family and are based on retention of liquids within a polymer matrix.[6] Lithium-polymer battery technology has progressed thanks to these achievements. The leakage issues occasioned by mechanical abuse or failure of battery enclosures have been considerably reduced since the polymer matrix efficiently entraps the liquid carbonates even at elevated temperatures. The mechanical integrity of the gel and swollen polymer electrolytes has also enabled the realization of non-trivial, free of form factor configurations including flexible,[7] stretchable,[8] transparent,[9] and paintable batteries.[10] Nonetheless, the contention of flammable and corrosive components raises concerns. While ionic liquids retain some of the standard electrolytes advantages, such as elevated ionic conductivity, further promoted by their chemical stability and especially, higher electrochemical working window of up to 6V, the rather elevated manufacturing and purification costs as well as increased viscosity have prevented their widespread adoption for LIBs.[11] Finally, it is worth mentioning that liquid based systems generally do not promote a stable electrode - electrolyte interphase owing to the unbound nature of the electrolyte and the continuous degradation of the battery performance is inevitable.

Solid-state electrolytes have thus become the keystone for the development of safer all-solid-state lithium devices. Ceramic and polymer electrolytes have been developed so far and display technologically relevant Li-ion conductivities.[12,13] However, the poor electrolyte - electrode interphase and especially the mechanical rigidity of ceramic electrolytes restrict their use to a limited number of battery configurations. By combining lightweight, easy implementation, flexibility and mechanical strength, solid polymer electrolytes appear to be an attractive alternative to the inorganic electrolytes.[14] Solid-state poly(ethylene oxide) (PEO) electrolytes are by far the most studied systems.[13] This originates from the simple fact that only PEO is capable to solvate considerable amounts of lithium salts and display relevant ionic conductivities in the solid state.[15] The major drawback however, is the low ionic conductivities attained at ambient temperature, rendering PEO unpractical for many applications including portable electronics. Since the solid-state lithium ion conduction occurs only in the amorphous phase, the room temperature dominant crystalline domains hamper dramatically the mobility of lithium ions through the electrolyte.[14] Several approaches have been developed so far to lower the melting point and enable the ambient temperature operation by adding organic plasticizers, inorganic fillers and nanoparticles.[16] Although the room temperature ionic conductivities have been significantly improved, the tradeoff was the degradation of mechanical properties. In a reverse approach, inorganic-organic hybrid materials using amorphous low molecular weight liquid PEG oligomer offer attractive ionic conductivities. The chemical anchor

to inorganic silica particles freezes somewhat the liquid behavior of the electrolyte. However, the mechanical properties obtained are similar to gel-like behavior.[17, 18]

Alternatively, poly(oligo(ethylene glycol) methacrylate) (POEGMA) exhibiting low glass transition temperature (T_G) has been proposed as a promising candidate to replace the traditional PEO electrolyte.[19] Unfortunately, POEGMA suffers of weak mechanical strength requiring mechanical reinforcement. To circumvent these drawbacks, various block copolymer architectures have been proposed that combine satisfactory mechanical properties and elevated ionic conductivity.[20, 21, 22] Despite, electrolytes with high molecular weight PEO blocks intrinsically limited the ionic conductivity given the PEO tendency to crystallize at room temperature, whereas non-optimized molecular backbone structures lead to lower than expected ionic conductivities. Here we show that by properly engineering the molecular structure of poly(styrene - ethylene oxide) based diblock-copolymers, a solid-state electrolyte displaying both, high ionic conductivities and enhanced mechanical strength, can be designed.

2. Experimental Section

Materials: Lithium perchlorate (battery grade, 99.99 %, Aldrich), 4,4'-Dinonyl-2,2'-dipyridyl (dNbpy, 97 %, Aldrich), Ethyl α-bromoisobutyrate (EBiB, 98%, Aldrich), N,N,N',N",N"-Pentamethyldiethylenetriamine (PMDETA, 99% Aldrich), Copper(I) bromide (CuBr, 99.999%, Aldrich), Copper(I) chloride (CuCl, >99.995%, Aldrich), $LiFePO_4$ (MTI corporation), Super C45 conductive carbon (MTI corporation), were used as received. (Oligo ethylene glycol) methyl ether methacrylate (OEGMA, M_n: 500 and 300 g/mol, Aldrich), Styrene (>99%, Aldrich) were filtered through activated basic alumina column prior to use. All other solvents and reagents were analytical grade and were used without further purification.

Synthesis of POEGMA homopolymer: A solution of benzyl bromoisobutyrate (BnBiB) (27 µL, 0.142 mmol, 1 eq.), $OEGMA_9$ (7.5 mL, 16.983 mmol, 120 eq.), dNbpy (118 mg, 0.290 mmol, 2.05 eq.) and absolute ethanol (5.4 mL, 40 wt%) was degassed three times by freeze-pump-thaw cycling. The degassed solution was introduced in Schlenk flask under argon atmosphere containing CuBr (20 mg, 0.142 mmol). The mixture was degassed three times by freeze-pump-thaw, filled with argon and stirred in oil bath at 60 °C for 30 min. The polymerization was stopped by cooling down at room temperature the Schlenk and exposing the catalyst to air. The reaction mixture is diluted in CH_2Cl_2 and filtered over neutral alumina. The solvent was removed under reduced pressure. The residue was diluted in methanol and then purified by dialysis (SpectraPor cut off 6000-8000 Da) in methanol over 48 h. The solvent is finally removed under reduced pressure and the residue dried under vacuum at 60 °C for 48 h, affording a clear oil. M_n (GPC) = 27000 g.mol^{-1}; Đ (GPC) = 1.26; ^{1}H NMR (500 MHz, $CDCl_3$) δ 7.5 (br s, 5H, Ar BnBiB), 4.2 (br s, 102H, CH_2 oligo ethylene glycol side chain), 3.9-3.2 (br m, 1530H CH_2 oligo ethylene glycol side chain), 2.2-0.8 (br m, 260H, CH_3-CH_2 backbone).

Synthesis of PS macroinitiator: A solution of EBiB (59 µL, 0.243 mmol, 1 eq.), styrene (18.6 mL, 162 mmol, 400 eq.), PMDETA (51 µL, 0.243 mmol, 0.6 eq.), and anisole (4.2 mL, 20 wt%) was degassed three times by freeze-pump-thaw cycling. The degassed solution was introduced in a Schlenk flask containing CuBr (29 mg, 0.202 mmol, 0.5 eq.). The solution was degassed three times by freeze-pump-thaw, filled with argon, stirred in oil bath at 90 °C over 15 h. The polymerization was stopped by cooling down the solution and exposing the catalyst to air. The reaction mixture was diluted with CH_2Cl_2 and passed through neutral alumina column. The solvent was removed under reduced pressure. The residue was precipitated twice in cold hexane, filtered and dried in vacuo at 35 °C for 15 h, affording a white powder. M_n (GPC) = 12200 g.mol^{-1}; Đ (GPC) = 1.09; ^{1}H NMR (500 MHz, $CDCl_3$) δ 7.3-6.3 (br m, 5 H, H_{Ar}), 2.3-1.2 (br m, 3H, CH-CH_2 backbone).

Typical procedure for PS-*b*-POEGMA block copolymer synthesis: A solution of PS-Br (530 mg, M_n: 12.2kg.mol^{-1}, PDI: 1.09), OEGMA (3.1 mL, 7.1 mmol, 164 eq.), dNbpy (36 mg, 0.089 mmol, 2.05 eq.), and anisole (3.4 mL, 50 wt%) was degassed three times by freeze-pump-thaw cycling. The degassed solution was introduced in a Schlenk flask containing CuCl (4 mg, 0.043 mmol, 1 eq.). The solution was degassed three times by freeze-pump-thaw, filled with argon, stirred in oil bath at 50 °C over 2h30. The polymerization was stopped by cooling down the solution and exposing the catalyst to air. The reaction mixture was diluted with CH_2Cl_2 and passed through neutral alumina column. The solvent was removed under reduced pressure. The residue was diluted in methanol and then purified by dialysis (SpectraPor cut off 6000-8000 Da) in methanol over 48 h. The solvent is finally removed under reduced pressure and the residue dried under vacuum at 60 °C for 48 h, affording an opalescent solid. M_n (GPC) = 52000 g.mol^{-1}; Đ (GPC) = 1.25; ^{1}H NMR (500 MHz, $CDCl_3$) δ 7.3-6.3 (br m, H_{Ar}), 4.2 (br s CH_2 oligo ethylene glycol side chain), 3.9-3.22 (br m CH_2 oligo ethylene glycol side chain), 2.0-0.7 (br m, $CHCH_3$-CH_2 backbone).

Electrolyte film preparation: The samples for cyclic voltammetry and electrochemical impedance spectroscopy thick film were prepared by drop casting method as follows. A solution 20 wt% of PS-*b*-POEGMA containing different ratio of $LiClO_4$ in THF was casted on a stainless steel electrode. The electrode was first dried in air for 4 h to remove excess solvent and then vacuum dried for 48 h at 60 °C. A typical thickness ranging from 80 to 160 µm is obtained.

$LiFePO_4$ electrode preparation: $LiFePO_4$/PS-*b*-$POEG_9MA$/Li metal cells were assembled and tested. The composite cathode was prepared by mixing $LiFePO_4$ 60 %wt, Super C45 25 %wt and PS-*b*-$POEG_9MA$ 15 %wt within few milliliters of 1-Methyl-2-pyrrolidinone during 12 h. The resulting slurry was casted onto carbon coated aluminum foil by using doctor blade technique followed by drying on a hot plate at 60 °C in air. The composite cathode with a thickness of 40 µm thick was obtained after drying at 60°C in vacuum for 24 h. The electrolyte was then slowly drop casted onto the composite cathode by using a PS-*b*-$POEG_9MA$, $LiClO_4$ (15:1 EO/Li) solution in THF. The cathode/electrolyte film was dried at 50°C in vacuum for 72h. Finally, $LiFePO_4$/PS-*b*-$POEG_9MA$/Li were assembled in Swagelock cell by pressing composite cathode-electrolyte against a lithium foil between two stainless steel electrodes. Batteries were cycled using an Arbin Instrument battery tester BT-2043 between 3 to 4 V at C/20 in thermostatic oven at 20°C and 40°C. C-rate measurements were conducted at 40 °C between C/20 to C.

Ionic conductivity: Ionic conductivities were measured by electrochemical impedance spectroscopy by using a Agilent LCR 4284A analyser. The electrochemical response of electrolyte is measured between two polished stainless steel electrodes in 10 Hz-1MHz frequency range with an AC excitation voltage of 5 mV. For liquid $POEG_9MA$, the electrolyte is poured between the two electrodes and the distance is held constant by using a 300 µm thick PTFE spacer. Arrhenius plot and temperature dependence

measurements were carried out from 20 to 90 °C by controlling the temperature with an Espec SH-261 oven. The temperature is gradually increased 10 by 10 °C and the samples stabilized 30 min prior any measurement.

Electrochemical stability window: The electrochemical stability window was determined by cyclic voltammetry by using a CHI660B instrument. Swagelock cells consisting of a thick film of polymeric electrolyte is sandwiched between a stainless steel working electrode and a lithium counter electrode. The cell is cycled between 0 V to 6 V *vs. Li+/Li* at a scan rate of 0.5 mV/s.

Mechanical Test: Shear rheological experiments were performed on a Kinexus Ultra (Malvern Instrument) rotational rheometer equipped with a heat exchanger. Measurements were carried out at 25°C, using a 8 mm plate–plate geometry. The gap was adjusted between 50 and 500 µm so that the geometry was completely filled. Normal forces were checked to be relaxed prior any measurement. Frequency sweeps were performed by recording the evolution of storage (*G'*) and loss (*G"*) moduli when decreasing the oscillation frequency (ω), under strain (γ_0) or stress (σ_0) amplitude that ensures a linear response from the materials. The critical shear strain and stress values (γ_0^c, σ_0^c) that separate the linear from the non-linear viscoelastic regime were here determined from strain–stress curves.

Differential Scanning Calorimetry measurement: DSC was performed on a Mettler Toledo DSC 822E at a rate of 5 °C/min between -110°C to 80°C, calibrated with indium standard.

Transmission Electron Microscopy: TEM was conducted on a Zeiss LEO 922 microscope operating at an accelerating voltage of 200 keV in bright field mode. Samples were prepared by drop casting of a 10 g/L PS-*b*-POEG$_9$MA $LiClO_4$ (15:1 EO/Li) solution onto a carbon-coated TEM grid, followed by staining with RuO_4 vapor during 5 min.

3. Results and discussion

3.1. Electrolyte design

The design strategy of the chemically anchored liquid-PEO electrolytes, integrating both high ionic conductivities and mechanical strength at room temperature is shown in Figure 1. The ion conduction in the designed bi-functional electrolyte is ensured by oligo(ethylene glycol) (OEG$_9$) with 9 units. In the free form, OEG$_9$ is a liquid with moderate viscosity (120 mPa.s) and relatively high ionic conductivity (~ 1mS/cm) at room temperature. The high ionic conductivity is ensured by free motion of ethylene oxide chains enabling non-restricted transport of Li^+ ions. The solvation of Li salt increases the viscosity thereby slightly affecting the ionic conductivity (see further discussion). Lower molar mass OEG's show decreased viscosity and respectively, higher ionic conductivities whereas increasing the mass reverses the trend and at high molar masses, or in other words for PEO, solid-state characteristics are being attained. It is thus of paramount interest to explore architectures that will benefit of the ionic conductivity of low molar mass OEG chains while being spatially constrained to yield mechanically rigid solid-state electrolytes.

By covalently linking OEG$_9$ to a polymethacrylic backbone, POEG$_9$MA is obtained. Although the new material preserves the ion conducting properties, it has the consistency of a highly viscous liquid with low structural integrity (Figure 1c). Drastic changes in mechanical properties are being noticed only after the incorporation of a high T_G polystyrene block (PS, Figure 1d). The material now

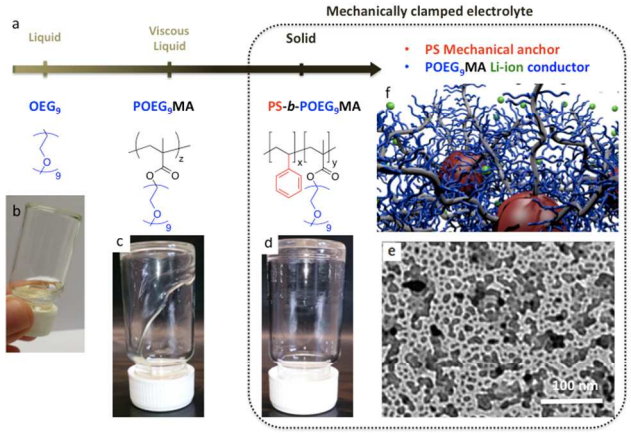

Figure 1 Functional hierarchy. (a) OEG$_9$-based electrolytes at different states. (b) Pristine OEG$_9$ has a fluid-like behavior. Covalently attaching OEG$_9$ to a methacrylate backbone results in a viscous liquid (c) whereas the addition of PS block progressively solidifies the matrix (d). Only small fraction of PS is necessary to anchor mechanically liquid-PEO based block copolymer electrolytes. The morphology of chemically anchored liquid-PEO was revealed by TEM (e) and consists of POEG$_9$MA entangled chains being attached to PS domains that act as chemical anchors as also schematically depicted in (f).

behaves as a rubbery solid whereas the ion-conduction performances are barely affecting (see further details/discussion). Relatively low PS content was found sufficient to trigger a microphase structuration due to the incompatibility between PS and POEGMA blocks. The morphology of the chemically anchored electrolyte is shown in Figure 1e and consists in glassy PS nanodomains uniformly dispersed within POEGMA amorphous phase. The characteristic dimensions of the ion-blocking PS domains are of the order of tens of nanometers, with no prominent continuous domains, resulting in lower ion percolation paths, ultimately leading to higher ionic mobility. At the same time, the glassy PS domains confer mechanical anchoring and integrity to the electrolyte whereas free chain motion of POEGMA ensures efficient ionic conduction. By precisely engineering the size and the composition of the block copolymer, superior mechanical performances are attained while not compromising the ionic conductivity as further detailed.

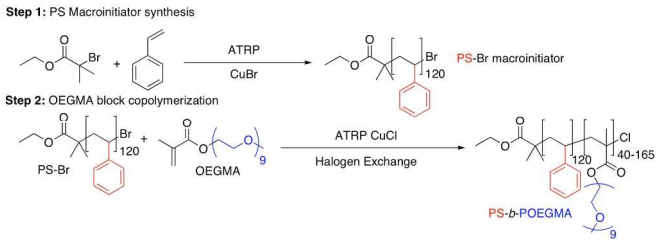

Figure 2 Synthesis strategy. The PS-*b*-POEGMA solid electrolytes have been synthesized through a simple two-step approach using ATRP.

The studied chemically anchored liquid-PEO block copolymers have been designed as to contain a low mass fraction of PS block to ensure dimensional stability and a major POEGMA ion conducting block to maximize the transport of lithium cations.[19] PS-*b*-POEGMA diblock copolymers were synthetized in a simple, two-step protocol through atom transfer radical polymerization (ATRP) (Figure 2).

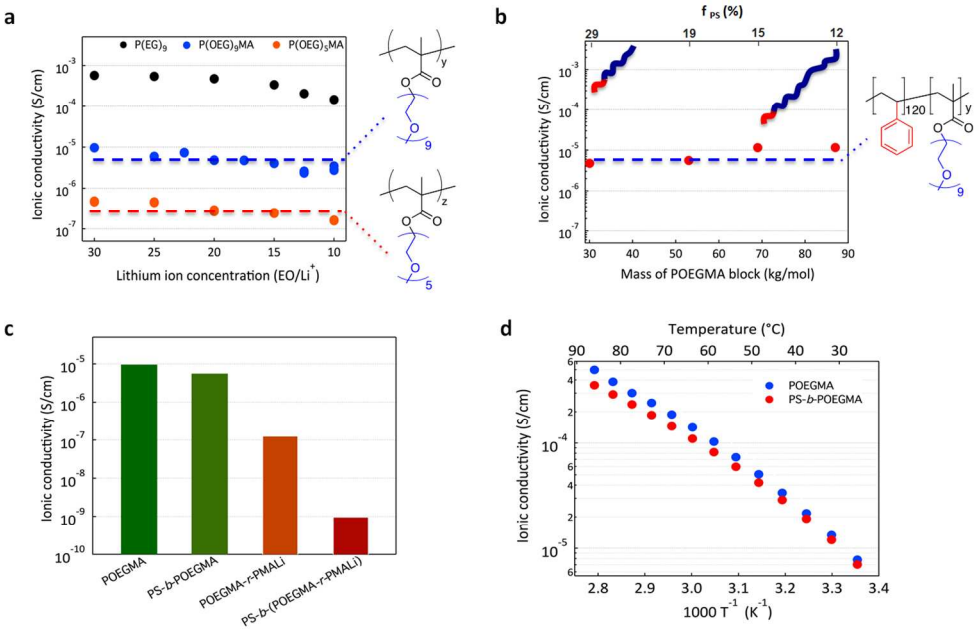

Figure 3. Ionic conductivity performances. (a) Lithium ion concentration dependence for OEG_9, $POEG_9MA$ and $POEG_5MA$ systems. (b) Influence of the PS block/unit length on the conductivity of the PS-*b*-$POEG_9MA$ solid electrolyte. (c) Comparison of doped and self-doped based electrolytes. (d) Temperature dependence of ionic conductivity for selected electrolytes

In the first step, a well-defined PS homopolymer with a narrow size distribution (Đ: 1.02) was obtained by ATRP. In a second step, the bromo-terminated PS acted as a macro-initiator for the polymerization of the POEGMA block. To precisely control the polymerization conversion (Đ < 1.3), the halogen exchange strategy was adopted.[23] Starting from a PS (DP_{PS} 120) macroinitiator, a library of PS_{120}-*b*-$[POEG_9MA]_y$ (where 40 < y ($DP_{POEG9MA}$) < 165) was synthetized and analyzed. $POEG_5MA$ and $POEG_9MA$ homopolymers have been also synthesized using ATRP to better understand the effect of the OEG side chain length and of the PS block incorporation (see Supplementary Information for further details about synthesis).

3.2. Ionic conductivities

The Li^+ conduction characteristics of the designed block-copolymer electrolytes are detailed in Figure 3. First, the influence of the OEG chain length and the addition of methacrylate backbone were investigated. The ionic conductivity versus lithium salt ($LiClO_4$) content is shown in Figure 3a. As expected, OEG_9 exhibits the highest conductivity (10^{-3} S/cm) given the good Li^+ solvation and mobility in the viscous liquid electrolyte. The conductivity decreases if higher amounts of salt are incorporated into the electrolyte, consistent with the ether crown ion chelation mechanism on account of increased number of complexes reducing thus the segmental motion of ethylene oxide chains, essential for fast ion conduction.[24]

The ionic conductivity has been found reduced in $POEG_9MA$ (Figure 3a). Nonetheless, the homopolymer exhibited competitive values of up to $1x10^{-5}$ S/cm at room temperature, higher than attained in semi-crystalline solid PEO electrolytes.[13,14] Unexpectedly, $POEG_5MA$ displayed much lower ionic conductivities although OEG_5 has intrinsically higher ion conduction than OEG_9. This originates from the inter-chain Li ion hopping transport mechanism. Although the OEG_5 chains are more mobile, covalent linking to the methacrylate backbone result in larger hopping distances and hence, lower conductivities. Increasing the molar mass of the OEG_n groups (n>9) is expected to lead to a decrease in the conductivity hence OEG chains will tend to crystallize.[25] Seemingly, OEG_9 is the best alternative and molecular modifications of the homopolymer backbone could be further applied to increase the ionic mobility.

Remarkably, the incorporation of the PS block has been found to minimally impact the ionic conductivity while drastically improving the mechanical properties. The influence of the PS block size on the ionic conductivity is shown in Figure 3b. For each case, a constant proportion of lithium perchlorate (20:1 EO/Li) was added to activate the electrolyte. By increasing the size of the $POEG_9MA$ block, only minor variations in the Li conduction were observed. Ionic conductivity of bout 1×10^{-5} S/cm were obtained for PS-*b*-$POEG_9MA$ electrolytes with $POEG_9MA$ blocks of 65k and 85k molar masses. For this configuration, the effect of the non ion-conductive PS block is completely diluted in the $POEG_9MA$ matrix, the electrolyte exhibiting similar performances to pristine $POEG_9MA$ while now behaving like a solid. At higher PS content, the ionic conductivity decreases only slightly, reaching a conductivity in excess of 5×10^{-6} S/cm for 30 kg/mol $POEG_9MA$ block. The volumic fraction of PS is more important and, although much better mechanical stability is expected, PS domains start to hinder Li motion in the electrolyte reducing the conductivity.[26]

In an attempt to gain deeper understanding and improve the ionic conductivity, self-doped chemically anchored liquid-PEO electrolytes have been also designed. By immobilizing the counter-ions to the polymer backbone their mobility is substantially reduced. As such, the Li^+ transport numbers could be as high as 1, effectively enabling single-ion conduction mechanism in such systems.[27] Nonetheless, much poorer electrolytic performances have been attained. As detailed in Figure 3c, self-doped electrolyte systems display 2 to 4 orders of magnitude lower ionic conductivities compared to doped systems, primarily due to strong chelating effect of the carboxylate groups.

To verify that the OEG phase in the chemically anchored solid-state electrolyte does not crystalize at ambient conditions, temperature dependent characteristics have been analyzed. The ionic conductivity follows a linear dependence function of temperature for both, $POEG_9MA$ and PS-*b*-$POEG_9MA$ systems, with activation energies

of 3,16 and 2,99 kJ/mol, respectively (Figure 3d). The absence of any sharp transitions implies no crystalline phase formation between 20 and 90°C as also confirmed by differential scanning calorimetry (see Supporting Information). In fact, DSC only shows a glass transition temperature of -70°C for POEG$_9$MA 40 kg/mol), clearly demonstrating that the PEO is in the amorphous phase at room temperature. A slight deviation in the conductivity behavior of both components can be observed at higher temperatures. The lower values for the PS-*b*-POEG$_9$MA are attributed to presence of the chemically anchored PS block known to have much higher glass transition values than the temperature range studied here.

3.3. Rheological measurements

To gain insight into the influence of the clamping PS blocks, the mechanical properties of the POEG$_9$MA homopolymer and PS-*b*-POEG$_9$MA block-copolymer were evaluated by rotational shear rheometry (Figure 4). The frequency dependence of the linear viscoelastic response of the pure POEG$_9$MA shows that the material behaves as a free-flowing Newtonian fluid. The presence of doping salt essentially restrains the chain motion, and thus, the final relaxation of the material. The latter still behaves as an un-entangled fluid, possessing a viscoelastic response through hydrodynamic and entropic effects, due to internal friction.

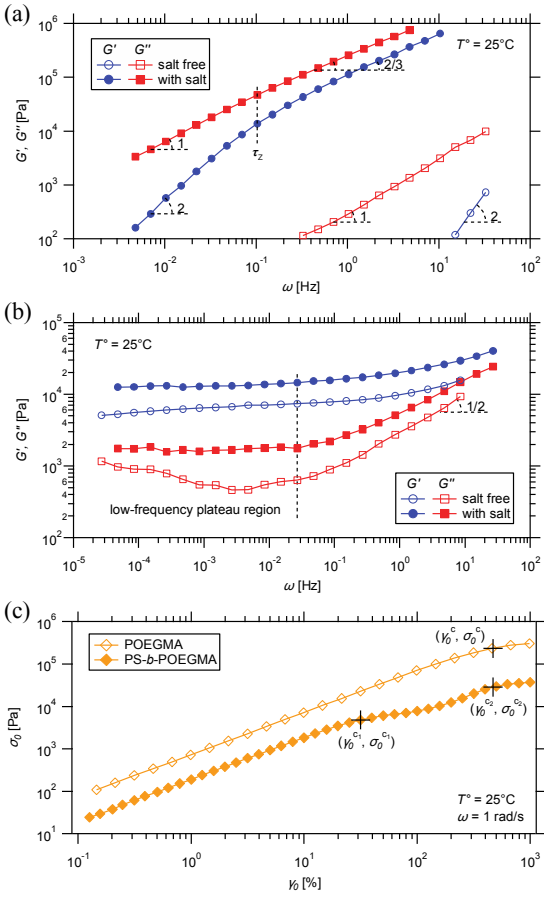

Figure 4. Mechanical performances. Frequency dependence of the linear dynamic viscoelastic response of (a) POEG$_9$MA, (b) PS-*b*-POEG$_9$MA doped and (c) Strain-stress curves of POEG$_9$MA, PS-*b*-POEG$_9$MA doped with 1/15 equivalents of $LiClO_4$.

In turn, the PS-*b*-POEG$_9$MA system also presents the characteristic short-range relaxation of POEG$_9$MA chains at high shear frequencies. Chain reptation within the material are however spatially confined so that the PS-*b*-POEG$_9$MA system does not display a terminal flow behavior. As such, the PS-*b*-POEG$_9$MA system behaves as a thermoplastic elastomer with a relatively low mechanical properties change upon Li cation doping. The mechanical strength of the Li^+-doped materials was finally tested by applying large shear forces to the samples. Practically, the shear amplitude is progressively increased on samples and their viscoelastic response monitored at a given angular frequency. For small oscillations, the response of both POEGMA and PS-*b*-POEGMA is expressed by a linear elastic behavior (Figure 4c), meaning that the integrity of the materials is only poorly affected by mechanical forces. Under large strain conditions, the viscoelastic response of the same materials deviates from linearity, with a clear distinction between the POEGMA and PS-*b*-POEGMA system. While the first shows a single yield point at around 500% strain, the second undergo multiple step yielding which is relevant for colloidal glasses. [28,29] Concretely, such a phenomenon can be ascribed to the disruption of attractive bonds between the glassy domains and subsequent breakdown of the latter into smaller components. The final yield of the material occurs at critical strain amplitude (γ_0^c) that matches the one of the Li-doped POEGMA electrolyte. However, the latter shows about one order of magnitude higher shear strength (σ_0^c) than the PS-*b*-POEGMA electrolyte, which can be rationally explained by the enhanced ability of the non-anchored material to relax mechanical forces.

To prove the applicability of the designed chemically anchored liquid-PEO based electrolytes for Li-ion storage, the electrochemical stability and battery prototypes have been analyzed. The cyclic voltammetry response of POEG$_9$MA and PS-*b*-POEG$_9$MA electrolytes is shown in Figure 5a and 5b, respectively. The studied cell consisted in a sandwiched polymer electrolyte between a stainless steel working electrode and a Li-metal anode and reference electrode. A wide electrochemical stability window is observed for both electrolytes. The cathodic peaks at potentials above 5.5V are mainly attributed to the decomposition of the $LiClO_4$ and oxidative corrosion of stainless steel working electrode. [30,31] Although less evident, PS-*b*-POEG$_9$MA shows much better passivating behaviour (as evidenced by the disappearance of the oxydation peak at ~ 5V) by promoting a stable solid electrolyte interphase (SEI). For potentials below 1.5V *vs.* Li/Li^+, considerable electrolyte decomposition can be observed for both electrolytes as evidenced by pronounced anodic peaks at ~ 1V and ~ 0.3V *vs.* Li/Li^+. The SEI formation cannot be avoided at such low potentials and is associated to complex surface reactions between the electrolyte components and the electrode materials (Li-metal in this case). [8] Whereas the first cycle shows congruent anodic behaviour for both electrolytes, subsequent cycling reveals major differences between them. In the case of liquid POEG$_9$MA, the formation of a dynamic, SEI can be observed over extended cycling. An unstable passivation film is formed and stripped at each cycles. The dimensional instability of the liquid gel electrolyte stimulates further this behaviour by continuously supplying a fresh electrolyte – electrode interface while accumulating solid reaction products in close vicinity. In the case of the chemically anchored liquid-PEO electrolyte, the corresponding anodic peak considerably diminishes as soon after the second scan, at the third scan the SEI formation being completely suppressed. This directly translates into the formation of a stable SEI passivating film only after a few cycles. As such, the structural rigidity of the PS-*b*-POEG$_9$MA electrolyte prevents the removal of the preformed SEI and thus avoiding the generation of a fresh electrode –

electrolyte interface. Hence a major issue in achieving efficient operation of Li-ion batteries is the design and implementation of electrode and electrolyte chemistries that will promote stable SEI for extended cycling, the formation of a stable protective interphase using PS-*b*-PEOG$_9$MA is highly beneficial as it can prevent electrode degradation and thus, increase the cycling stability and Coulombic efficiency.

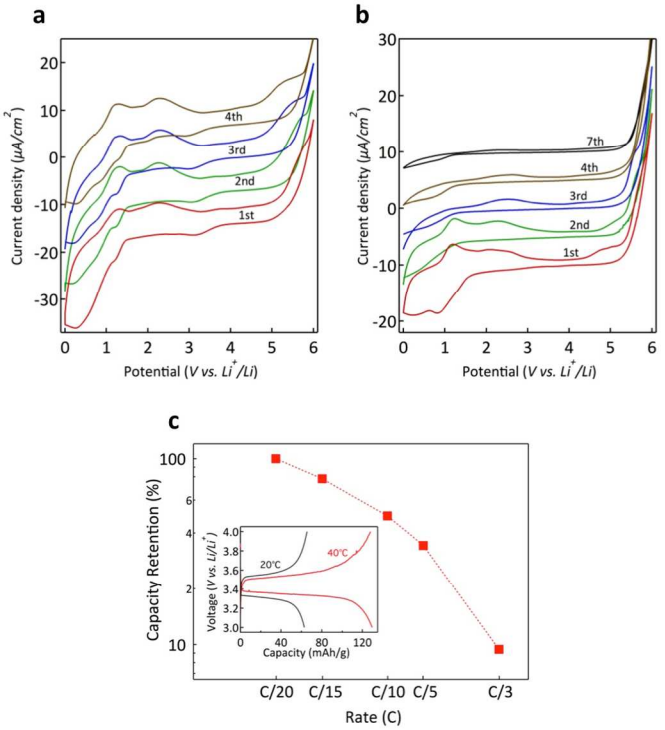

Figure 5. Electrochemical performances. Cyclic voltammetry response of (a) POEG$_9$MA and (b) PS-*b*-POEG$_9$MA solid-state electrolytes at a scan rate of 0.5mV/s. The curves are shifted by 5 μA/cm^2 for clarity. The current onset above 5V is mainly due to the electrolyte salt decomposition and stainless steel oxidative corrosion. (c) Rate performance of a LiFePO$_4$/PS-*b*-POEG$_9$MA/Li-metal solid-state cell cycled at 40°C (1C rate corresponds to a current density of 160 mA/g). Inset: charge-discharge profiles at 20°C and 40°C at a current density of 8 mA/g.

Finally, a solid state battery prototype was built using the PS-*b*-POEG$_9$MA electrolyte. Figure 5c shows the rate performance and charge-discharge profiles of the all-solid-state battery consisting of a LiFePO$_4$ cathode and a Li-metal anode. The composite electrode was approximately 40 μm thick and the thickness of the electrolyte film was 400 μm. At a current density of 8 mA/g (corresponding to a cycling rate of C/20) the battery delivers more than 130 mAh/g at 40°C. The stored energy diminishes when operating the battery at 20°C nonetheless, the cell still delivers 60mAh/g. This is also accompanied by considerable electrode polarization significative of lower ionic conductivity and associated concentration polarization. At 40°C the battery displays satisfactory rate performance with half of the nominal capacity being retained when cycled at C/5 rate. We expect that upon further technical optimization, for example, by reducing the porosity of the composite electrode and especially dimnishing the thickness of the electrolyte layer, enhanced cycling efficiency and rate performance could be obtained. Nonetheless, the proof-of-concept all-solid-state battery with chemically anchored liquid-PEO electrolyte is clearly demonstrated.

4. Conclusions

To conclude, starting from a liquid OEG$_9$ building block, we design a chemically anchored liquid-PEO electrolyte exhibiting outstanding performance at room temperature. To merge together high Li^+ conductivity with mechanical strength, a block copolymer strategy was developed where minor polystyrene blocks are successfully found to freeze the dimensional stability while not affecting the ion conduction. Furthermore, by changing the relative size of the two blocks, the mechanical and ion conduction properties can be finely tuned. To meet high ionic conductivity for practical requirements, the PS-*b*-POEG$_9$MA side chain length has been designed such as to achieve ionic conductivities in excess of 10^{-5} S/cm. The system is also found to display a wide electrochemical stability window above 5 V *vs.* Li^+/Li, which makes the developed electrolyte applicable not only to the conventional Li-ion technology but also to the developing high voltage cathode materials. The dimensional integrity of the chemically anchored liquid electrolyte promotes much stable behavior at anodic potentials enabling efficient passivation and limited electrode and electrolyte degradation. Owing to these outstanding properties for reliable and safe devices, PS-*b*-POEG$_9$MA paves the way to the design and implementation of new all-solid-state lithium ion batteries.

Acknowledgements

The authors are grateful Walloon Region for financial funding in the frame of the Batflex and Batwal projects. AV acknowledges FRS-FNRS for financial support. J.B. thanks F.R.I.A. for Ph.D. thesis grant

Notes and references

[a] BSMA/IMCN, Université catholique de Louvain, Place Louis Pasteur, 1 1348 Louvain-la-Neuve, Belgium.
[b] Electrical Engineering, Université catholique de Louvain, Place du Levant 3, 1348 Louvain-la-Neuve, Belgium.

[1] J. B. Goodenough, Y. Kim, *Chem. Mater.* **2010**, *22*, 587.
[2] M. Armand, J. M. Tarascon, *Nature* **2008**, *451*, 652.
[3] A. Vlad, N. Singh, J. Rolland, S. Melinte, P. M. Ajayan, J.-F. Gohy, *Sci. Rep.* **2014**, *4*, 4315.
[4] J. M. Tarascon, M. Armand, *Nature* **2001**, *414*, 359.
[5] B. Scrosati, J. Garche, *J. Power Sources* **2010**, *195*, 2419.
[6] W. A. Van Schalkwijk, B. Scrosati, *Advances in lithium ion batteries* (Kluwer Academic Publishers/Plenum, New York, 2002).
[7] A. Vlad, A. L. M. Reddy, A. Ajayan, N. Singh, J.-F. Gohy, S. Melinte, P. M. Ajayan, *Proc. Natl. Acad. Sci.* **2012**, *109*, 15168.
[8] S. Xu, Y. Zhang, J. Cho, J. Lee, X. Huang, L. Jia, J. A. Fan, Y. Su, J. Su, H. Zhang, H. Cheng, B. Lu, C. Yu, C. Chuang, T.-I. Kim, T. Song, K. Shigeta, S. Kang, C. Dagdeviren, I. Petrov, P. V. Braun, Y. Huang, U. Paik, J. A. Rogers, *Nat. Comm.* **2013**, *4*, 1543.
[9] Y. Yang, S. Jeong, L. Hu, H. Wu, S. W. Lee, Y. Cui, *Proc. Natl. Acad. Sci.* **2011**, *108*, 13013.
[10] N. Singh, C. Galande, A. Miranda, A. Mathkar, W. Gao, A. L. M. Reddy, A. Vlad, P. M. Ajayan, *Sci. Rep.* **2012**, *2*, 481.
[11] M. Armand, F. Endres, D. R. Macfarlane, H. Ohno, B. Scrosati, *Nat. Mater.* **2009**, *8*, 621.
[12] G. Y. Adachi, N. Imanaka, H. Aono, *Adv. Mater.* **1996**, *8*, 127.
[13] W. H. Meyer, *Adv. Mater.* **1999**, *10*, 439.
[14] E. Quartarone, P. Mustarelli, *Chem. Soc. Rev.* **2011**, *40*, 2525.
[15] F. Croce, G. Appetecchi, L. Persi, B. Scrosati, *Nature* **1998**, *394*, 456.
[16] E. Quartarone, P. Mustarelli, A. Magistris, *Solid State Ionics* **1998**, *110*, 1.

[17] J. Fan, S. R. Raghavan, X.-Y. Yu, S. A. Khan, P. S. Fedkiw, J. Hou, G. L. Baker, *Solid State Ionics* **1998**, *111*, 117.
[18] L. M. Bronstein, R. L. Karlinsey, K. Ritter, C. G. Joo, B. Stein, J. W. Zwanziger, *J. Mater. Chem.* **2004**, *14*, 1812.
[19] A. V. G. Ruzette, P. P. Soo, D. R. Sadoway, A. M. Mayes, *J. Electrochem. Soc.* **2001**, *148*, 537.
[20] R. Bouchet, S. Maria, R. Meziane, A. Aboulaich, L. Lienafa, J.-P. Bonnet, T. N. T. Phan, D. Bertin, D. Gigmes, D. Devaux, R. Denoyel, M. Armand, *Nat. Mater.* **2013**, *12*, 452.
[21] W.-S. Young, W.-F. Kuan, T. H. Epps, *J. Polym. Sci. B: Polym. Phys.* **2013**, *52*, 1.
[22] P. E. Trapa, B. Huang, Y.-Y. Won, D. R. Sadoway, A. M. Mayes, *Electrochem. Solid-State Lett.* **2002**, *5*, A85.
[23] K. Matyjaszewski, D. A. Shipp, J. Wang, T. Grimaud, T. E. Patten, *Macromolecules* **1998**, *31*, 6836.
[24] N. A. Stolwijk, C. Heddier, M. Reschke, M. Wiencierz, J. Bokeloh, G. Wilde, *Macromolecules* **2013**, *46*, 8580.
[25] I. Yukio, K. Keiichi, M. Katsuki, K. Tetsuichi, *J. Mater. Sci.* **1987**, *22*, 1845.
[26] Q. Li, E. Wood, H. Ardebili, *Appl. Phys. Lett.* **2013**, *102*, 243903.
[27] D. R. Sadoway, *J. Power Sources* **2004**, *129*,1.
[28] N. Koumakis, G. Petekidis, *Soft Matter* **2011,** *7*, 2456.
[29] K. Pham, G. Petekidis, D. Vlassopoulos, S. Egelhaaf, W. Poon, P. Pusey,. *J. Rheol.* **2008,** *52*, 649.
[30] M. Armand, *Solid State Ionics* **1983**, *9*, 745.
[31] S.-T. Myung, Y. Hitoshi, Y.-K. Sun, *J. Mater. Chem.* **2011**, *21*, 9891.

Electronic Supplementary Information (ESI) available

See DOI: 10.1039/b000000x/

TOC entry:

A mechanically clamped liquid-poly(ethylene oxide) electrolyte that combines high ionic conductivity and dimensional integrity of a solid material is designed.

TOC graphic: